Interocular suppression in normal and amblyopic vision: Spatio-temporal properties

Pi-Chun Huang
Department of Psychology, National Cheng Kung University, Tainan, Taiwan
McGill Vision Research, Department of Ophthalmology, McGill University, Montreal, Quebec, Canada

Daniel H. Baker
School of Life & Health Sciences, Aston University, Birmingham, UK

Robert F. Hess
McGill Vision Research, Department of Ophthalmology, McGill University, Montreal, Quebec, Canada

We measured the properties of interocular suppression in strabismic amblyopes and compared these to dichoptic masking in binocularly normal observers. We used a dichoptic version of the well-established probed-sinewave paradigm that measured sensitivity to a brief target stimulus (one of four letters to be discriminated) in the amblyopic eye at different times relative to a suppression-inducing mask in the fixing eye. This was done using both sinusoidal steady state and transient approaches. The suppression-inducing masks were either modulations of luminance or contrast (full field, just overlaying the target, or just surrounding the target). Our results were interpreted using a descriptive model that included contrast gain control and spatio-temporal filtering prior to excitatory binocular combination. The suppression we measured, other than in magnitude, was not fundamentally different from normal dichoptic masking: lowpass spatio-temporal properties with similar contributions from both surround and overlay suppression.

Keywords: interocular suppression, amblyopia, dichoptic masking, dynamic

Citation: Huang, P.-C., Baker, D. H., & Hess, R. F. (2012). Interocular suppression in normal and amblyopic vision: Spatio-temporal properties. *Journal of Vision*, *12*(11):29, 1–12, http://www.journalofvision.com/content/12/11/29, doi:10.1167/12.11.29.

Introduction

The ability to detect targets shown monocularly (i.e., to one eye only) can be severely impaired by competing textures shown to the other eye. These dichoptic masking effects are strongest when the characteristics of target and mask are similar (e.g., Baker & Meese, 2007; Legge, 1979) but can remain substantial when they differ, e.g., in orientation (Meese & Baker, 2009). Neurophysiological studies provide evidence that an active process of interocular suppression, taking place in the primary visual cortex, underpins the behavioral phenomena (Li, Peterson, Thompson, Duong, & Freeman, 2005; Sengpiel & Vorobyov, 2005). But although much is known about the spatial properties and tuning of these effects, little work has focused on their temporal dynamics.

Here, we address this omission by modifying a well-established paradigm developed for investigating the dynamics of luminance adaptation in the retina. In the probed sine-wave paradigm (see Wolfson & Graham, 2006, for a recent review), sensitivity to a luminance-defined target is measured as a function of a sinusoidally varying background luminance. We extend this paradigm here in two ways. First, the dynamic mask stimulus is presented to the opposite eye from the target, ensuring that any masking effects are cortical and not retinal in origin (see also Wolfson & Graham, 2001). Second, we consider texture-defined masks ($1/f$ noise) as well as modulations of luminance.

This dynamic dichoptic masking paradigm allows us to ask several questions about the temporal properties of interocular suppression. If suppression were instantaneous, there should be no lag between the mask phase and its effect on the target. This is an unlikely scenario, given that some processing of the mask must take place before it suppresses the target, and this will introduce a temporal lag that should be behaviorally apparent. Furthermore, temporal filtering will tend to blur the mask signal across time (e.g., Apthorp, Cass, & Alais, 2011), which might reduce the temporal modulation of the masking effect at higher temporal frequencies.

doi: 10.1167/12.11.29 Received April 27, 2012; published October 31, 2012 ISSN 1534-7362

As well as informing about interocular suppression in normal observers, this paradigm is of particular utility for investigating amblyopia. Monocular developmental abnormalities (e.g., strabismus, anisometropia, or cataract) often result in a reduced sensitivity of the affected eye, even when the causative pathology is corrected. One potential cause of this deficit is increased suppression from the good eye onto the bad (e.g., Harrad & Hess, 1992; Jampolsky, 1955; Travers, 1938), and it seems plausible that temporal abnormalities might be involved in this (e.g., if the mask signal was pooled over an unusually long period). The precise source of this (hypothetical) extra suppression is rarely made explicit, but since thresholds in the amblyopic eye remain elevated even in the absence of a high contrast mask (i.e., when the fellow eye views mean luminance) one possible culprit is suppression from low spatial frequency tuned mechanisms that respond to uncontoured fields (Yang & Stevenson, 1999). Alternatively, some reports have found no evidence for increased interocular suppression in amblyopes once the differences in monocular sensitivity are factored out (Baker, Meese, & Hess, 2008).

We set out to answer three related questions concerning amblyopic suppression: (a) Are its temporal dynamics lowpass or bandpass? (b) Does suppression have spatial lowpass or bandpass tuning (Freeman and Jolly, 1994)? (c) Is amblyopic suppression fundamentally different, other than in magnitude (e.g., in any of the above), from normal dichoptic masking (Baker et al., 2008; Freeman & Jolly, 1994; Harrad & Hess, 1992)?

We carried out four variations of the dichoptic probed sine-wave experiment in both normal and amblyopic observers. We first used a full-field fractal noise mask that varied sinusoidally in contrast and measured its effect on detection thresholds for monocular letter stimuli shown to the opposite eye. We then repeated the experiment using either a small disc of noise or the full mask with a central disc removed to compare overlay and surround masks (Petrov, Carandini, & McKee, 2005). Finally, we measured thresholds when the mask was a dichoptic modulation of mean luminance. Computational modeling facilitates estimation of the temporal dynamics of interocular suppression and informs as to the likely locus of the amblyopic deficit.

Methods

Apparatus

The stimuli were generated using Psykinematix (Beaudot, 2009) and presented using virtual reality goggles (eMagin Z800 3DVisor) to permit independent stimulation of the left and right eyes (pilot experiments confirmed that thresholds for one eye were independent of the luminance shown to the other [patched] eye). The refresh rate of the goggles was 60 Hz, and the mean luminance was 160 cd/m^2. No Gamma correction was necessary due to the luminance linearity of organic light-emitting diode (OLED) goggles (see figure 2 of Black, Maehara, Thompson, & Hess, 2011).

Stimuli

Targets were letters of the alphabet (Z, X, C, or V) presented monocularly on a mean luminance background for one frame (16.67 ms). The target luminance was always an increment relative to the background (i.e., white letters), and was manipulated to estimate the minimum increment required for detection. We express letter detection thresholds using the Weber (or delta) contrast ratio expressed as a percentage: $C_{\%} = 100 \times (L_{target} - L_{background})/L_{background}$, or in logarithmic units (decibels; $C_{dB} = 20\log_{10}[C_{\%}]$). The target letters subtended approximately 5.18° of visual angle and were presented on a background that was 22.68° wide in each direction.

There were four mask types, all of which were presented dichoptically (i.e., in the opposite eye to the target). The full-field mask was an isotropic noise texture with an amplitude spectral falloff proportional to $1/f$ (previously shown to produce strong masking, Hansen & Hess, 2012, and maximal interocular suppression, Baker & Graf, 2009), where f is the spatial frequency (note that the letter targets had a similar amplitude spectrum, Gervais, Harvey, & Roberts, 1984; Solomon & Pelli, 1994). The same noise sample was used for each block but rotated randomly (in steps of 90°) on each trial. This mask was square with a width of 20.86° and a maximum RMS contrast of 28 dB (24%). The small mask was a circular section of the noise texture (radius 2.25°) in the center of the display. The surround mask was the difference between the full-field and small masks, i.e., a square of noise texture with a circular hole in the center. Finally, we modulated the mean luminance displayed to the nontarget eye between (nominally) zero and twice the mean luminance (320 cd/m^2), which constituted our fourth mask type.

Each mask type was modulated sinusoidally at 1, 2, or 3 Hz, with negative values constituting phase reversals for the contrast conditions and luminances below the mean (i.e., decrements) for the luminance mask. We also measured thresholds for discrete mask presentations, where the mask was displayed at a fixed contrast (−100%, −50%, 0%, 50%, 100% of the maximum) for 50 ms. This is referred to as the *impulse* condition and had a nominal temporal frequency of 0

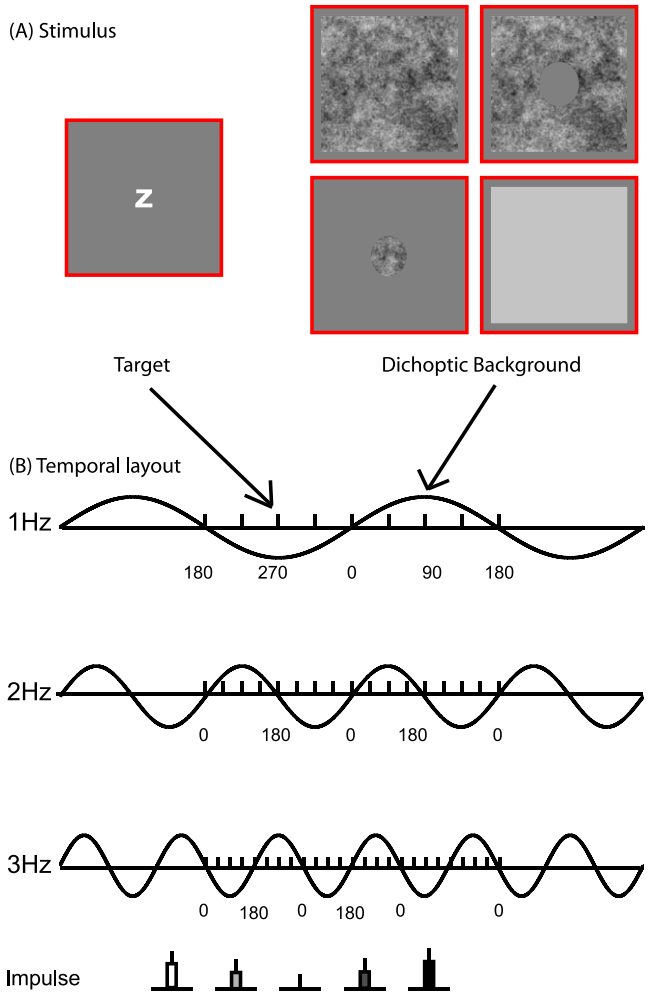

Figure 1. (A) An example of the stimulus arrangement used in the experiment. One of the eyes was shown a flickering background (mask) and the other eye was shown a letter (target). Four types of masks were used: full-field mask, surround mask, small mask, and luminance mask. (B) Temporal profile used in the experiment. The sinusoidal curve shows the luminance/contrast of the flickering background and the short vertical lines showed eight possible phases when the target (letter) was presented. Each trial contained one letter at a single randomly-chosen time.

Hz. A schematic diagram representing the experimental conditions is shown in Figure 1.

Procedure

In the main experiments, the observer's task was to identify the target letter (Z, X, C, or V) shown on each trial by pressing the corresponding symbol on the keyboard. The dichoptic mask was presented for 2 s and the target was presented in the time window between 0.5 and 1.5 s from the start of the mask presentation. Target contrast was determined by a two-down-one-up staircase (in steps of 2.5 dB) and auditory feedback was given to indicate correctness of response. The staircase terminated after six upward reversals; the last five reversals were averaged to calculate the thresholds. At least two staircase measures were collected to determine the threshold for each condition. Threshold elevation was calculated by subtracting (in dB units) the baseline threshold (with no mask) from the masked detection threshold.

We ensured that the images shown to the two eyes were correctly aligned for each observer before the start of each experimental session. A nonius figure, featuring a binocular square with vertical monocular lines above and below the center, was adjusted using the keyboard so that the two lines (shown to opposite eyes) were collinear. The positions obtained from this procedure were used to present the stimuli in each session.

For the full field mask (luminance and contrast), eight staircases (eight sample phases for a given temporal frequency) were interleaved in one session lasting around 12 minutes. For the small and surround masks (where ocular alignment was particularly important), four staircases (four randomly selected sample phases for a given temporal frequency) were interleaved in one session and the other four phases were run in the following session to minimize any potential drift in ocular alignment for the amblyopic participants. The alignment task described above was repeated before each experimental session and typically returned stable alignment values for all observers throughout 1–2 hours of data collection for a given day.

Analysis

Threshold elevation was plotted as a function of mask phase. We fitted the data with a descriptive model using a least squares method. Because negative mask contrasts constitute a phase reversal in our paradigm, we used a full-wave rectified sinusoidal function, defined as,

$$T_{dB} = \alpha + |\beta \sin(2\pi\theta - \Phi)|, \quad (1)$$

where θ is the phase angle of the mask, and α, β, and Φ are free parameters. The α parameter provides a vertical (DC) offset from zero (i.e., no masking) and the β parameter determines the amplitude of the modulation. Both of these parameters are scaled in dB units. The Φ parameter offsets the function horizontally and is scaled in degrees of phase of the temporal modulation.

Observers

Seven amblyopic and four normal observers participated in the experiments. All observers wore their

normal optical correction during testing. Clinical details for each of the strabismic amblyopes are shown in Table 1.

Results

Baseline thresholds are shown in Figure 2 for all observers, plotted as the more sensitive eye (lower thresholds) on the ordinate and the less sensitive eye (higher thresholds) on the abscissa. It is clear that normal observers (filled symbols) had approximately equal sensitivity, whereas some amblyopes (open symbols) showed a substantial deficit in the affected eye for the letter identification task. We used these baselines to calculate the size of the masking effect (threshold elevation) for each mask condition.

Threshold elevation for the full-field noise mask is shown in Figures 3a–d, averaged across the left and right eyes of four normal observers. The impulse condition (Figure 3a) produced between 0 and 6 dB of threshold elevation, depending on mask contrast. When a temporal component was added, this raised the baseline of the masking function above zero and reduced the amplitude of the modulation (Figures 3b–d). There is also evidence of a lateral offset that increases with temporal frequency: The function in Figure 3d is shifted rightward in phase by around 45°. Similar patterns were evident in the data for individual observers (not shown).

Threshold elevation for the surround mask is shown in Figures 3e–h, averaged across the left and right eyes of three normal observers. The impulse condition (Figure 3e) produced a small threshold elevation at the highest mask contrasts (denoted as 90° and 270° for comparison with the temporally modulated conditions). When a temporal component was added, it did not substantially affect the pattern of masking relative to the impulse condition (Figures 3f–h). Unlike for the full-field mask, there was no elevation of the baseline or reduction in amplitude for dichoptic surround masks. We return to this surprising finding in the Discussion.

Threshold elevation for the small noise mask is shown in Figures 3i–l, averaged across the left and right

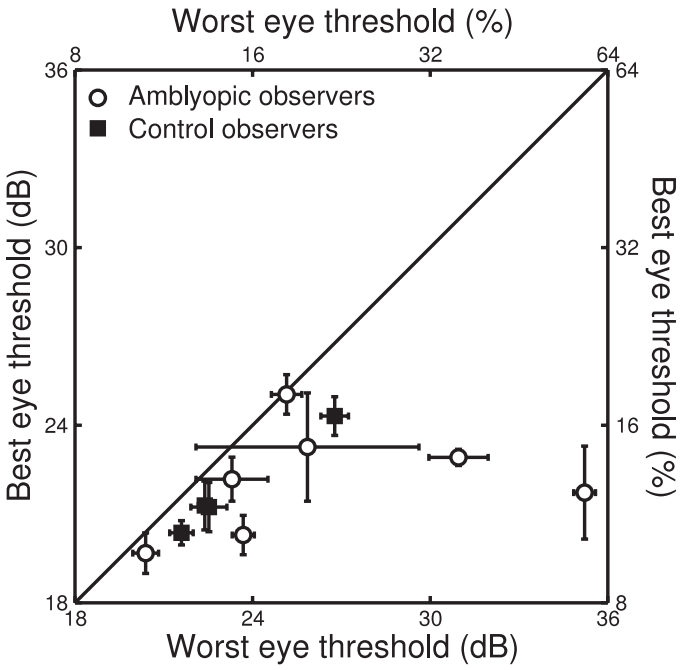

Figure 2. Scatterplot showing baseline thresholds in each eye for eleven observers. Open circles indicate amblyopic observers (n = 7) and filled squares indicate normal controls (n = 4). Each point is the mean of the baselines across each experiment (typically four for most observers), with error bars showing ±1 *SE* of the mean.

Observer	Age/gender	Strabismus	Eye	Acuity	First detected	Patching therapy	Surgery	Mask conditions
AS	33/F	Right ET	R	20/125	3 yrs		None	F, L
		20°	L	20/25		None		
CD	28/F	Right XT	R	20/25	<2 yrs		Age 2	F, Sm, Su, L
		20°	L	20/20		3 yrs		
KM	52/F	Right XT	R	20/32	6 mon		Mon 6 Age 4	F, Sm, Su, L
		20°	L	20/15		None		
EV	20/F	Right XT	R	20/200	<3 yrs		2 times	F, Sm, Su, L
		15°	L	20/32		Occasionally (ages 3–7)		
AR	51/M	Left XT	R	20/20	6 yrs		None	F, L
		3°	L	20/50		None		
LP	48/F	Right XT	R	20/160	11 yrs		None	F, Sm, Su, L
		8°	L	20/20		For 6 mon		
CH	30/F	Left ET	R	20/20	3–4 yrs		Yes	F, Sm, Su, L
		8°	L	20/400		Yes		

Table 1. Clinical details of amblyopic observers.

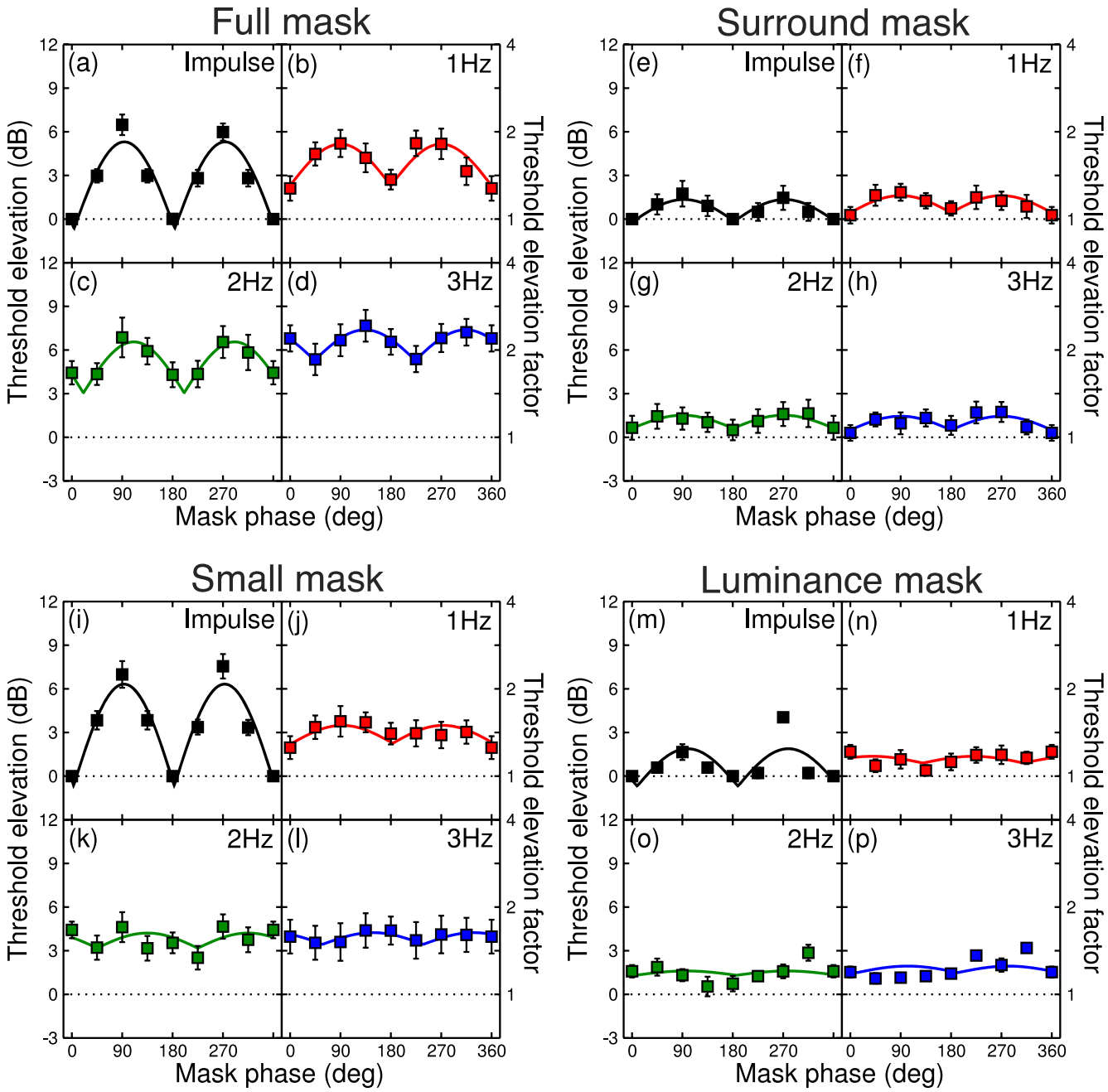

Figure 3. Threshold elevation for four mask types as a function of mask phase at the time of target presentation: (a–d) the full-field noise mask, (e–h) surround mask, (i–l) small mask, and (m–p) luminance mask. Each set of four panels shows results for the different temporal conditions described in the text. Data are averaged across the left and right eyes of the normal observers, with error bars showing ±1 *SE* of the mean. Curves are the best fits of Equation 1 with three free parameters per temporal condition.

eyes of three normal observers. This is qualitatively similar to the condition with a full-field mask, with slightly weaker masking at the higher temporal frequencies. At 3 Hz, there was again a lateral offset of around 45°.

Figures 3m–p show threshold elevation for the luminance mask, averaged across the left and right eyes of three normal observers. The impulse condition (Figure 3m) produced between 0 and 4 dB of threshold elevation, depending on mask contrast, with the strongest masking occurring when the mask's luminance contrast was −100% (i.e., at a nominal phase of 270°, which is a decrement relative to the background luminance of the target eye). When a temporal component was added, this raised the baseline of the masking function by around 2 dB, independent of the temporal frequency and strength of the mask (Figures 3n–p). This DC offset, combined with weak dynamic

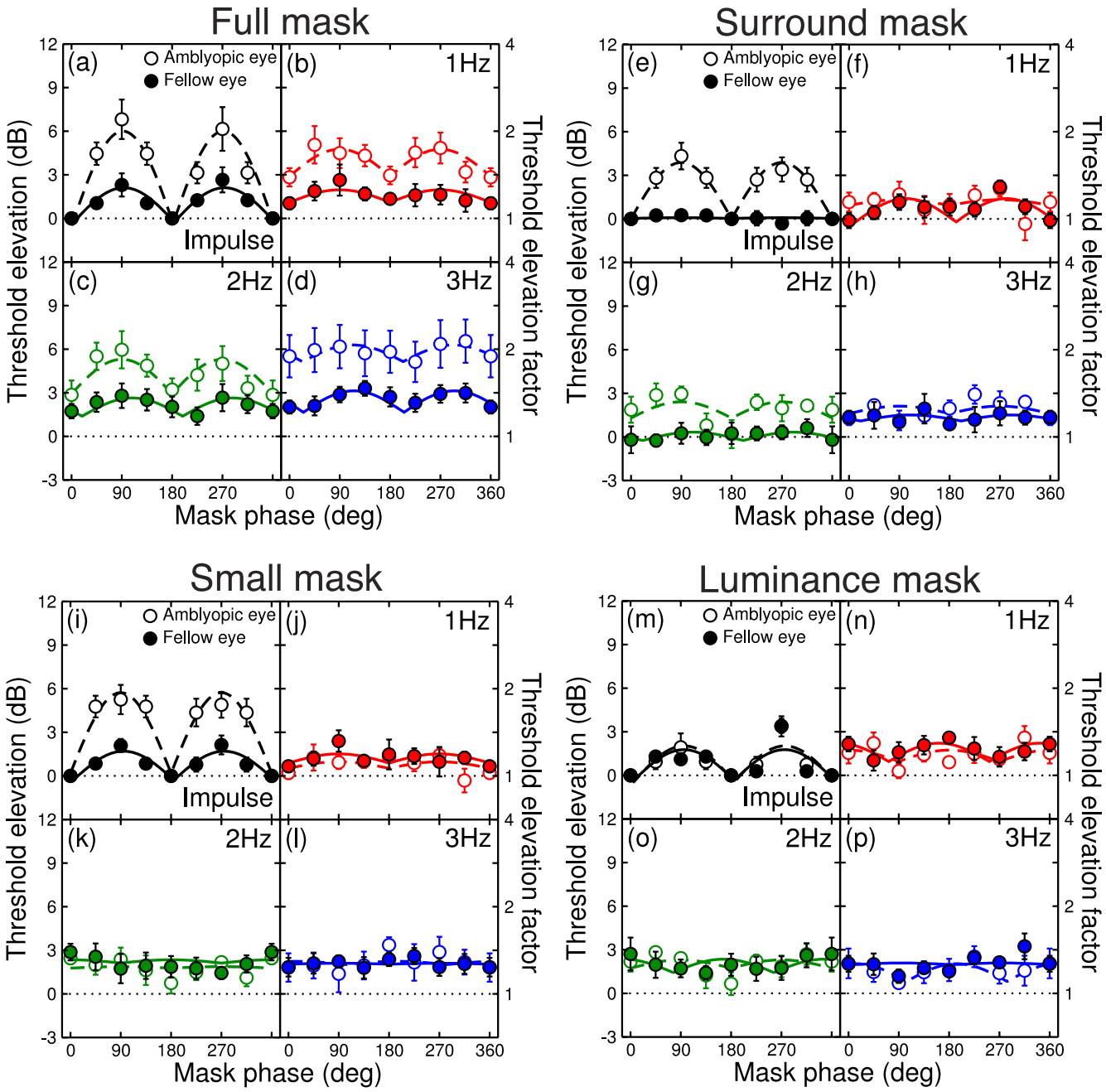

Figure 4. Threshold elevation for four types of masks in amblyopic observers in a similar format to Figure 3. Open symbols represent threshold elevation in the amblyopic eye with masks presented to the fellow eye. Filled symbols represent threshold elevation in the fellow eye when masks were presented to the amblyopic eye.

modulation, is consistent with previous findings using a similar paradigm (Wolfson & Graham, 2001).

Complementary results for amblyopic observers are shown in Figure 4. For the full-field mask (Figures 4a–d), the masking effect, averaged over seven amblyopic observers, followed a similar pattern as for normal observers, particularly in the amblyopic eye (open symbols) where threshold elevation is comparable to those in Figures 3a–d. This suggests that suppression of the amblyopic eye by the fellow eye is no stronger than in the normal observers. Threshold elevation in the fellow eye was weaker (filled symbols), consistent with an attenuation of the mask signal in the amblyopic eye prior to interocular suppression (see Baker et al., 2008). The dynamics of interocular suppression appear very similar in amblyopes and normal observers.

The effect of a surrounding noise mask, averaged across five amblyopic observers, is shown in Figures 4e–h. There was clear modulation of thresholds in the amblyopic eye, stronger than in normal observers

(Figures 3e–h). Masking in the fellow eye was weak (Figures 4f, h) or absent (Figures 4e, g), most likely also due to attenuation of the masking signal in the amblyopic eye.

Threshold elevation for the small noise mask is shown in Figures 4i–l, averaged over five amblyopic observers. As with normal observers, the impulse condition (Figure 4i) was similar to that for the full-field mask (Figure 4a). When a temporal component was added, masking became weaker in the amblyopic eye but stayed roughly the same in the fellow eye (Figures 4j–l).

For the luminance mask (Figures 4m–p), there was no clear difference in threshold elevation between the amblyopic and fellow fixing eyes. Temporal modulation introduced only very small changes in the amount of masking and the data from this experiment are very similar to those of the control subjects (Figures 3m–p).

We also summarize the main trends by comparing the parameters obtained by fitting Equation 1 to the data, as described in the following section.

Descriptive model

We fitted a full-wave rectified sine-wave to the data of each observer and to the group average data for the normal and amblyopic observers. Since there were no major differences between the left and right eyes of the normal observers, these data were also averaged before fitting. Parameters for each of the four experiments are shown in Figure 5, with lines representing fits to the average data. Parameters from fits to the data of individual observers were, on average, similar in form (not shown).

As expected from an inspection of Figures 3a–d and Figures 4a–d, there were clear trends for each of the three free parameters for the full-field noise mask. The DC offset (α) increased with temporal frequency (Figure 5a) from an expected value of zero in the impulse (0 Hz) condition (because all of the data are normalized to the 0° point in this condition, where the mask contrast was zero), consistent with the upward shift of the masking data minima. The amplitude of the masking functions was weakest for high temporal frequencies (Figure 5e), as evidenced by the downward trend for this parameter (β). The phase offset (Φ) increased with temporal frequency (0° phase offset is also expected for the impulse condition, though this was not fixed in the model fitting), reaching a maximum of around 45° in the 3 Hz condition (Figure 5i).

Parameters for the small noise mask (Figures 5c, g, k) were broadly similar to those for the full-field mask (Figures 5a, e, i). The surround mask produced masking that was weaker in terms of DC offset (Figure 5b) and amplitude (Figure 5f), with no clear phase offset (Figure 5j). This implies that the lateral suppression which presumably causes dichoptic surround masking is less profound than the direct interocular suppression from overlaid masks (Figures 5c, g, k) and may be subject to different temporal constraints, perhaps associated with a different level of processing. The luminance condition (Figure 5d, h, l) also showed poor dynamics (small DC offset and amplitude).

The negligible amplitude in this condition (Figure 5h) is responsible for the essentially random phase offset parameters (Figure 5l). Offsets could not be estimated reliably without a large enough modulation.

In general, parameters were comparable for the control subjects (solid lines) and the bad eyes of the amblyopes (dashed lines). This confirms that amblyopic suppression from the good eye to the bad did not differ from normal suppression in either its magnitude or its temporal dynamics. Amblyopic suppression from the bad eye to the good was often weaker in terms of both amplitude and DC offset (dotted line, top and middle rows) but did not show a consistent difference in phase offset (dotted line, bottom row).

Functional model

The principal trends apparent in Figures 3–5 (at least for the full and small masks) are that the threshold elevation functions shift upwards and to the right with increasing temporal frequency whilst also reducing in amplitude. In this section we develop a functional model that can quantitatively account for this behavior. In brief, we combine a standard contrast gain control equation (Foley, 1994; Legge & Foley, 1980) with a low-pass-filtered, temporally delayed masker signal. The temporal offset accounts for the phase shift in the masking functions and the low-pass filtering produces the upward shift and reduction in modulation depth (amplitude).

The model response is given by

$$resp = \frac{C^p}{Z + C^q + wM(t)^q}, \quad (2)$$

where C is target contrast (expressed in linear units as a percentage) the exponents p and q take on typical values (Legge & Foley, 1980) of 2.4 and 2, respectively, the saturation constant Z has an arbitrary value of 0.7, and the weight of suppression (w) has a value of 4. The masking term, M, at time t, is defined as

$$M(t) = |\sin(2\pi tf)| * 0.1e^{\frac{-(t-\tau)^2}{2\sigma^2}}, \quad (3)$$

where t is time in seconds, f is the mask temporal frequency in Hz, $*$ denotes convolution, and τ and σ are the offset and standard deviation (respectively) of the

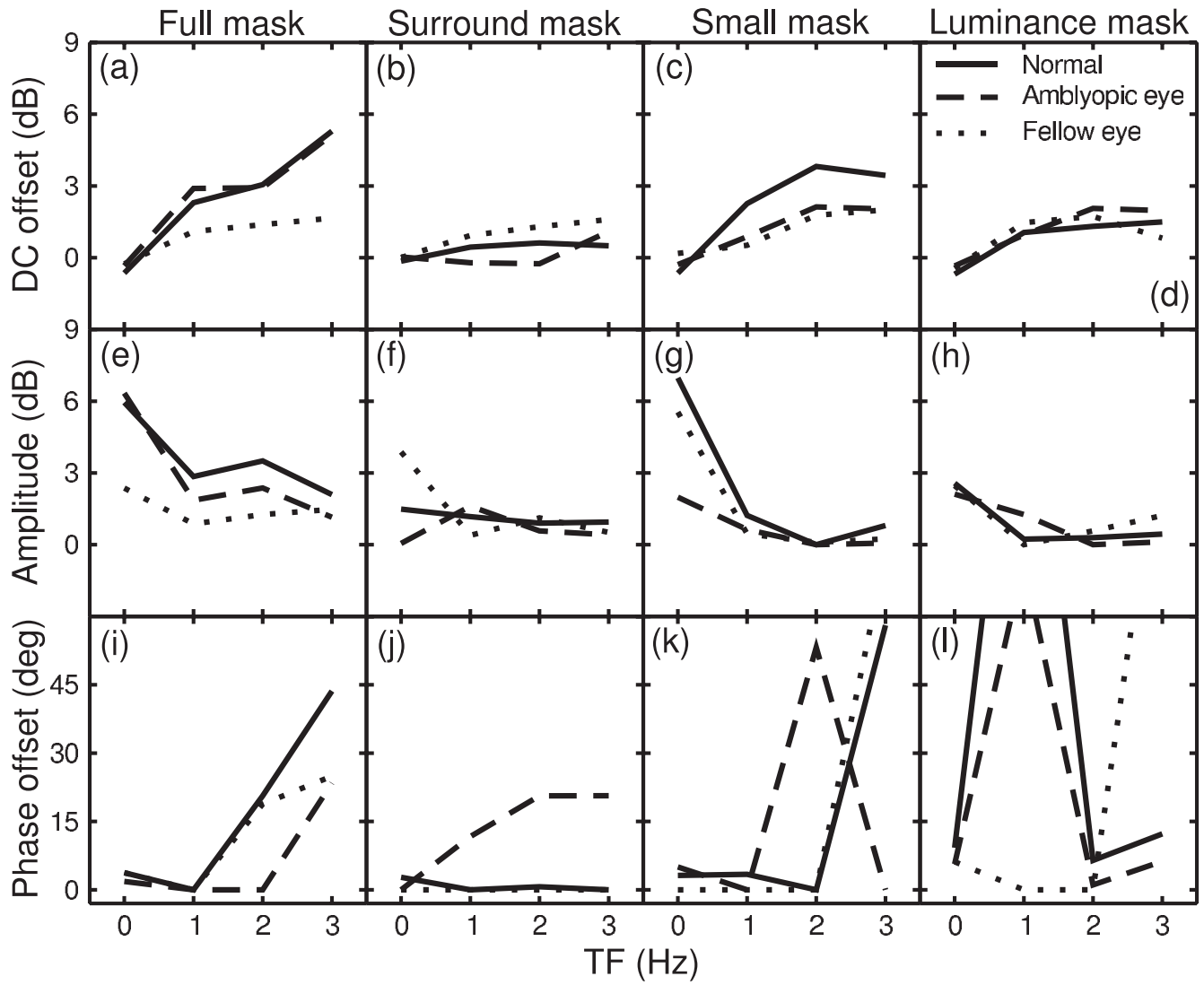

Figure 5. Summary of parameters of Equation 1 for fits to the averaged data of four experiments. Columns represent different experiments, specified in the column headings. Rows represent different parameters for the DC offset (α; top row), amplitude of the modulation (β; middle row), and phase offset (Φ; bottom row). The data for normal observers (solid lines) were averaged across eye and observer before fitting. The data for amblyopic observers (dashed and dotted lines) were averaged across observers, but analyzed individually for the amblyopic and fellow eyes.

Gaussian convolution kernel. Threshold is obtained when $resp_{\text{target}} - resp_{\text{null}} = k$, where $k = 0.2$, with the equations solved numerically to find estimates of threshold at each mask phase. For the impulse (0 Hz) condition, M is simply the discrete mask contrast displayed in the experiment.

The behavior of this model is shown in Figure 6 (solid curves) for parameter values that produce plausible behavior ($\tau = 40$ ms; $\sigma = 50$ ms, corresponding to a full-width-at-half-height of ~120 ms for the convolution kernel). The model captures all of the main features of the data described above. The DC and phase offsets of the masking functions increase whilst the amplitude decreases towards the higher temporal frequencies. The convolution has a greater effect at higher temporal frequencies because Equation 3 is defined in terms of time rather than phase. This model is consistent with interocular suppression being delayed by around 40 ms and blurred in the temporal domain. Note that although the model uses a rectified sine-wave, convolution with the Gaussian kernel smooths the function to more closely approximate a nonrectified sine wave, particularly at higher temporal frequencies (e.g., Figure 6d).

We also show how the behavior changes when the mask signal is attenuated by a factor of two (Figure 6, dotted curves). This simulates well the masking functions for the fellow eyes of amblyopes (solid curves in Figure 4) on these threshold-normalized axes.

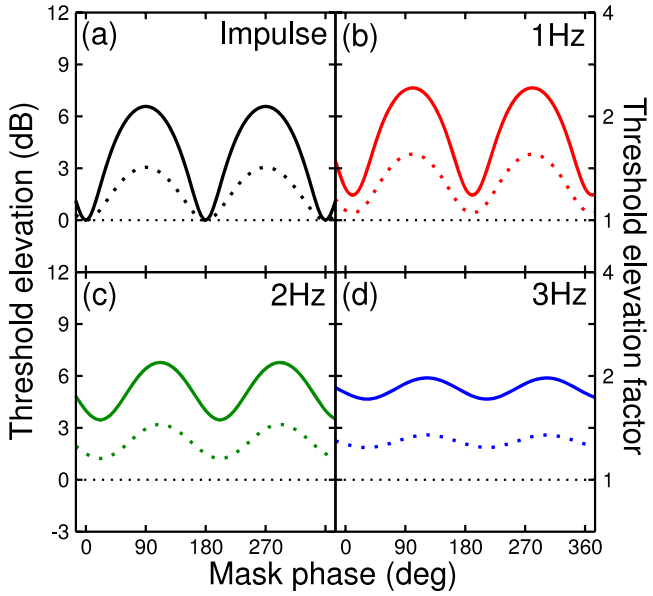

Figure 6. Behavior of a functional model of interocular suppression, in which the mask signal is blurred and offset in time. Solid curves simulate normal observers and dotted curves show how the behavior changes when the mask signal is attenuated by a factor of two (simulating the fellow eye data for amblyopic observers, see Figure 4). See text for details.

General discussion

We measured dichoptic threshold elevation caused by four types of dynamic mask. Thresholds were elevated by up to 6 dB (a factor of two), with the suppression being greatest at times coincident with high mask contrast (or substantial luminance deviation). At higher temporal frequencies of mask oscillation, there was evidence of temporal delay and blurring in the suppressive signal. Masking was similar for normal observers and in the affected eye of amblyopes. The normal eye of amblyopic observers exhibited weaker masking.

Temporal properties of masking, facilitation, and rivalry

Several estimates exist for the timecourses of related suppressive and facilitatory phenomena. Cass and Alais (2006) used dynamic (rotating) flanking stimuli to estimate the speed at which facilitative interactions travel in cortex. They isolated two temporal processes; one that appears to propagate through cortex at around 10 cm/s and the other that has a delay of 20–80 ms.

Wong, Roeber, and Freeman (2010) used a rapid serial visual presentation task to measure the timecourse of both facilitation and suppression for grating stimuli. They analyzed their data using a reverse correlation technique and isolated a rapid facilitatory process (<100 ms) and a slower suppressive process (100–300 ms) that had a similar timecourse within and between the eyes. They also used a forward masking technique to show that interocular masking remained fairly constant from 10–50 ms before decaying.

In binocular rivalry, travelling waves of inhibition (or disinhibition) have been measured spreading slowly through the cortex, both psychophysically (Kang, Heeger, & Blake, 2009; Wilson, Blake, & Lee, 2001) and using fMRI (Lee, Blake, & Heeger, 2005). These waves propagate across the cortex at around 2 cm/s and across visual space at around 3.65°/s (Wilson et al., 2001), with some individual differences (Kang et al., 2009). This relatively sluggish suppression (at least compared with facilitation) is consistent with our finding that dichoptic masking lags in time and may involve the same neural substrate.

Amblyopic suppression has similar dynamics to normal dichoptic masking, being temporally lowpass with a temporal cutoff in the vicinity of 3 Hz. Surprisingly, we found no evidence of temporal offsets using our surround configuration. This could imply a very rapid process of suppression, or alternatively, a more general, nonsensory (perhaps attention-related) source of threshold elevation such as increased uncertainty (Pelli, 1985) or distraction (Kontsevich & Tyler, 1999). Given the typically weak surround masking in the fovea for grating masks (which appears to be isotropic, see Meese, Challinor, Summers, & Baker, 2009), this latter possibility is not unlikely.

Masking from very low spatial frequency channels

We found a weak masking effect caused by dichoptic luminance modulation (Figures 3m–p) consistent with previous results for detecting a luminance-decrement probe (Wolfson & Graham, 2001). Given the spatially low-pass properties of this mask and also our target letters (which were not DC balanced), this is perhaps unsurprising as it could be mediated by suppression between low spatial frequency sensitive mechanisms (e.g., Yang & Stevenson, 1999). However, it should be noted that the task involved letter discrimination, not merely detection, and that the mechanisms underlying discrimination performance are thought to be spatially bandpass (Solomon & Pelli, 1994). Therefore the suppression would need to be spatially lowpass and cross-channel in character in order to influence a bandpass letter detecting mechanism centered at a higher spatial scale. Note also that for high spatial frequency targets, increasing the luminance input to the

nontarget eye can actually improve sensitivity (Denny, Frumkes, Barris, & Eysteinsson, 1991).

Our finding that amblyopes do not show different levels of masking in their normal and amblyopic eyes in the luminance condition (Figures 4m–p) is consistent with the amblyopic deficit being confined to higher spatial frequencies for many observers (Hess & Howell, 1977). In other words, there is no amblyopic attenuation in the very low spatial frequency channels that mediate masking from mean luminance. Freeman and Jolly (1994) report a similar luminance masking effect in amblyopia using an acuity task (comparing acuity when the nontarget eye was shown mean luminance to when it was dark). Interestingly, there was no such effect for their normal observers, which might indicate that the masking from mean luminance extends to higher spatial frequencies in amblyopes. Our results cannot distinguish this point, however, as we used only mid-spatial frequency letter stimuli as targets.

Appropriateness of our descriptive model

Equation 1 uses a full-wave rectified sine wave to describe the threshold elevation data. For the contrast-defined masks (i.e., the noise textures) this is appropriate because negative values of the sine wave correspond to phase reversals of the mask, which should not produce different levels of masking from positive values. However, for the luminance modulation, positive mask levels are increments and negative levels are decrements relative to the mean (background) luminance of 160 cd/m^2. Given that increments and decrements appear to behave very differently in binocular vision (Anstis & Ho, 1998; Baker, Wallis, Georgeson, & Meese, 2012) we might expect them to produce different amounts of suppression. Visual inspection of the luminance data was suggestive of greater masking in the negative phase (e.g., decrement portion) of the oscillation for both normal and amblyopic observers (see in particular the points at 270° in Figures 3m and 4m). However, the level of suppression was too weak in this condition to satisfactorily constrain a more complex model. For the parameters of interest here (amplitude, DC, and phase offsets), Equation 1 was sufficient.

Models of amblyopic contrast vision

In previous work (Baker et al., 2008), a model of normal binocular contrast vision (Meese, Georgeson, & Baker, 2006) was lesioned in various ways to attempt to simulate amblyopic deficits in contrast detection and discrimination. The most successful modification involved an early attenuator in the amblyopic eye, prior to any suppressive or excitatory binocular interactions. This approach accounted well for pedestal masking in several arrangements (Baker et al., 2008) and has since been successfully extended to other paradigms (Huang, Zhou, Lu, & Zhou, 2011).

In the context of the present study, an early attenuator would (a) reduce the suppression of the fellow eye by the amblyopic eye, accounting for the weaker masking in this condition (see filled symbols in Figure 4) and (b) leave suppression of the amblyopic eye by the fellow eye unaffected once differences in detection threshold are factored out (i.e., by calculating threshold elevation; see open symbols in Figure 4). The dotted curves in Figure 6 demonstrate the former behavior for a two-fold attenuation of the mask signal in the amblyopic eye. Although the functional model we propose above uses a single stage gain control (for transparency), we obtained comparable behavior (not shown) using a multistage binocular model (Meese et al., 2006). Thus, the results here are not inconsistent with the architecture proposed by Baker et al. (2008), with the new insight that interocular suppression is blurred and delayed in the temporal domain.

Huang et al. (2011) also required increased interocular suppression from the fellow to the amblyopic eye in order to account for their data. We find no evidence for this here, perhaps because of the different tasks used in the two studies (phase and contrast matching vs. letter identification) or the different amblyopic subgroups used (anisometropic vs. strabismic amblyopes). We note, however, that Baker et al. (2008) demonstrated that for their dichoptic pedestal masking paradigm, differences in the weight of interocular suppression did not lead to differences in the level of masking between the two eyes (see their figure 7). Thus, whether such differences exist could not be revealed by their pedestal masking technique.

Implications for amblyopia therapy

Recently, attempts have been made to address the binocular deficit in amblyopia directly with specific dichoptic therapy aimed at strengthening binocular fusion and reducing suppression (Hess, Mansouri, & Thompson, 2010a, 2010b, 2011; To et al., 2011). The present results are consistent with our previous findings (Baker et al., 2008) that amblyopic suppression is similar to normal dichoptic masking and support our working hypothesis that amblyopic binocular combination is structurally similar to that of the normal visual system, the main exception being that there is an attenuator in the monocular amblyopic pathway (perhaps in the lateral geniculate nucleus, see Hess, Thompson, Gole, & Mullen, 2009). This results in an imbalance in the monocular inputs as well as reduced

suppression of the fixing eye's input prior to excitatory combination (Baker et al., 2008). The effect of this is to render a structurally binocular circuit functionally monocular. That such a simple imbalance can have such a dramatic functional effect gives hope to therapies designed to actively boost the influence of the amblyopic eye within the binocular process.

Conclusions

Amblyopic suppression has similar dynamics to that of normal dichoptic masking; it is temporally lowpass with a temporal acuity around 3 Hz. Spatially, it may be lowpass though our results are not definitive on this issue. In some cases its magnitude is greater than that expected of normal dichoptic masking.

Acknowledgments

Supported by Grant MOP53346 from the CIHR to RFH and Grant EP/H000038/1 from the EPSRC (UK).

Commercial relationships: none.
Corresponding author: Pi-Chun Huang.
Email: pichun_huang@mail.ncku.edu.tw.
Address: Department of Psychology, National Cheng Kung University, Tainan City, Taiwan.

References

Anstis, S., & Ho, A. (1998). Nonlinear combination of luminance excursions during flicker, simultaneous contrast, afterimages and binocular fusion. *Vision Research, 38*, 523–539.

Apthorp, D., Cass, J., & Alais, D. (2011). The spatial tuning of "motion streak" mechanisms revealed by masking and adaptation. *Journal of Vision, 11*(7): 17, 1–16, http://www.journalofvision.org/content/11/7/17, doi:10.1167/11.7.17. [PubMed] [Article]

Baker, D. H., & Meese, T. S. (2007). Binocular contrast interactions: Dichoptic masking is not a single process. *Vision Research, 47*, 3096–3107.

Baker, D. H., Meese, T. S., & Hess, R. F. (2008). Contrast masking in strabismic amblyopia: Attenuation, noise, interocular suppression and binocular summation. *Vision Research*, *48*, 1625–1640.

Baker, D. H., & Graf, E. W. (2009). Natural images dominate in binocular rivalry. *Proceedings of the National Academy of Sciences of the United States of America*, *106*, 5436–5441.

Baker, D. H., Wallis, S. A., Georgeson, M. A., & Meese, T. S. (2012). Nonlinearities in the binocular combination of luminance and contrast. *Vision Research, 56*, 1–9.

Beaudot, W. H. A. (2009). Psykinematix: A new psychophysical tool for investigating visual impairment due to neural dysfunctions. *Vision: The Journal of the Vision Society of Japan, 21*, 19–32.

Black, J. M., Maehara, G., Thompson, B., & Hess, R. F. 2011. A compact clinical instrument for quantifying suppression. *Optometry and Vision Science, 88*, 334–342.

Cass, J., & Alais, D. (2006). The mechanisms of collinear integration. *Journal of Vision, 6*(9):5, 915–922, http://www.journalofvision.org/content/6/9/5, doi:10.1167/6.9.5. [PubMed] [Article]

Denny, N., Frumkes, T. E., Barris, M. C., & Eysteinsson, T. (1991). Tonic interocular suppression and binocular summation in human vision. *The Journal of Physiology*, *437*, 449–460.

Foley, J. M. (1994). Human luminance pattern-vision mechanisms: Masking experiments require a new model. *Journal of the Optical Society of America A, 11*, 1701–1719.

Freeman, A. W., & Jolly, N. (1994). Visual loss during interocular suppression in normal and strabismic subjects. *Vision Research*, *34*, 2043–2050.

Gervais, M. J., Harvey, L. W., & Roberts, J. O. (1984). Identification confusions among letters of the alphabet. *Journal of Experimental Psychology: Human Perception and Performance, 10*, 655–666.

Hansen, B. C., & Hess, R. F. (2012). On the effectiveness of noise masks: Naturalistic vs. unnaturalistic image statistics. *Vision Research, 60*, 101–113.

Harrad, R. A., & Hess, R. F. (1992). Binocular integration of contrast information in amblyopia. *Vision Research, 32*, 2135–2150.

Hess, R. F., & Howell, E. R. (1977). The threshold contrast sensitivity function in strabismic amblyopia: Evidence for a two type classification. *Vision Research, 17*, 1049–1055.

Hess, R. F., Mansouri, B., & Thompson, B. (2010a). A binocular approach to treating amblyopia: Antisuppression therapy. *Optometry and Vision Science, 87*, 697–704.

Hess, R. F., Mansouri, B., & Thompson, B. (2010b). A new binocular approach to the treatment of amblyopia in adults well beyond the critical period

of visual development. *Restorative Neurology and Neuroscience, 28*, 1–10.

Hess, R. F., Mansouri, B., & Thompson, B. (2011). Restoration of binocular vision in amblyopia. *Strabismus, 19*, 110–118.

Hess, R. F., Thompson, B., Gole, G., & Mullen, K. T. (2009). Deficient responses from the lateral geniculate nucleus in humans with amblyopia. *European Journal of Neuroscience, 29*(5), 1064–1070.

Huang, C.-B., Zhou, J., Lu, Z.-L., & Zhou, Y. (2011). Deficient binocular combination reveals mechanisms of anisometropic amblyopia: Signal attenuation and interocular inhibition. *Journal of Vision, 11*(6):4, 1–17, http://www.journalofvision.org/content/11/6/4, doi:10.1167/11.6.4. [PubMed] [Article]

Jampolsky, A. (1955). Characteristics of suppression in strabismus. *Archives of Ophthalmology, 54*, 683–696.

Kang, M.-S., Heeger, D., & Blake, R. (2009). Periodic perturbations producing phase-locked fluctuations in visual perception. *Journal of Vision, 9*(2):8, 1–12, http://www.journalofvision.org/content/9/2/8, doi:10.1167/9.2.8. [PubMed] [Article]

Kontsevich, L. L., & Tyler, C. W. (1999). Distraction of attention and the slope of the psychometric function. *Journal of the Optical Society of America A, 16*, 217–222.

Lee, S.-H., Blake, R., & Heeger, D. J. (2005). Traveling waves of activity in primary visual cortex during binocular rivalry. *Nature Neuroscience, 8*, 22–23.

Legge, G. E. (1979). Spatial frequency masking in human vision: Binocular interactions. *Journal of the Optical Society of America A, 69*, 838–847.

Legge, G. E., & Foley, J. M. (1980). Contrast masking in human vision. *Journal of the Optical Society of America, 70*, 1458–1471.

Li, B., Peterson, M. R., Thompson, J. K., Duong, T., & Freeman, R. D. (2005). Cross-orientation suppression: Monoptic and dichoptic mechanisms are different. *Journal of Neurophysiology, 94*, 1645–1650.

Meese, T. S., Georgeson, M. A., & Baker, D. H. (2006). Binocular contrast vision at and above threshold. *Journal of Vision, 6*(11):7, 1224–1243, http://www.journalofvision.org/content/6/11/7, doi:10.1167/6.11.7. [PubMed] [Article]

Meese, T. S., Challinor, K. L., Summers, R. J., & Baker, D. H. (2009). Suppression pathways saturate with contrast for parallel surrounds but not for superimposed cross-oriented masks. *Vision Research, 49*, 2927–2935.

Meese, T. S., & Baker, D. H. (2009). Cross-orientation masking is speed invariant between ocular pathways but speed dependent within them. *Journal of Vision, 9*(5):2, 1–15, http://www.journalofvision.com/content/9/5/2, doi:10.1167/9.5.2. [PubMed] [Article]

Pelli, D. G. (1985). Uncertainty explains many aspects of visual contrast detection and discrimination. *Journal of the Optical Society of America A, 2*, 1508–1532.

Petrov, Y., Carandini, M., & McKee, S. (2005). Two distinct mechanisms of suppression in human vision. *The Journal of Neuroscience, 25*, 8704–8707.

Sengpiel, F., & Vorobyov, V. (2005). Intracortical origins of interocular suppression in visual cortex. *The Journal of Neuroscience, 25*, 6394–6400.

Solomon, J., & Pelli, D. G. (1994). The visual filter mediating letter identification. *Nature, 369*, 395–397.

To, L., Thompson, B., Blum, J., Maehara, G., Hess, R. F., & Cooperstock, J. (2011). A game platform for treatment of amblyopia. *IEEE Transactions on Neural Systems & Rehabilitation Engineering, 19*, 280–289.

Travers, T. (1938). Suppression of vision in squint and its association with retinal correspondence and amblyopia. *British Journal of Ophthalmology, 22*, 577–604.

Wilson, H. R., Blake, R., & Lee, S. H. (2001). Dynamics of travelling waves in visual perception. *Nature, 412*, 907–910.

Wolfson, S. S., & Graham, N. (2001). Processing in the probed-sinewave paradigm is likely retinal. *Visual Neuroscience, 18*, 1003–1010.

Wolfson, S. S., & Graham, N. (2006). Forty-four years of studying light adaptation using the probed-sinewave paradigm. *Journal of Vision, 6*(10):3, 1026–1046, http://www.journalofvision.org/content/6/10/3, doi:10.1167/6.10.3. [PubMed] [Article]

Wong, E. M. Y., Roeber, U., & Freeman, A. W. (2010). Lengthy suppression from similar stimuli during rapid serial visual presentation. *Journal of Vision, 10*(1):14, 1–12, http://www.journalofvision.org/content/10/1/14, doi:10.1167/10.1.14. [PubMed] [Article]

Yang, J., & Stevenson, S. B. (1999). Post-retinal processing of background luminance. *Vision Research, 39*, 4045–4051.